

## Article

# Elemental Carbon Observed at a Peri-Urban Forest Site near the Seoul Metropolitan Area as a Tracer of Seasonal Haze Occurrence

Jeeyoung Ham <sup>1,2</sup>, Inseon Suh <sup>1,3</sup>, Meehye Lee <sup>1,\*</sup>, Hyunseok Kim <sup>4,5,6,7</sup>  and Soyoung Kim <sup>8</sup>

<sup>1</sup> Department of Earth and Environmental Sciences, Korea University, Seoul 02841, Korea; uwayes@korea.kr (J.H.); suhis@ecobrain.net (I.S.)

<sup>2</sup> National Air Emission Inventory and Research Center, Cheongju 28166, Korea

<sup>3</sup> Ecobrain Co., Ltd., Seoul 05855, Korea

<sup>4</sup> Department of Agriculture, Forestry and Bioresources, College of Agriculture and Life Sciences, Seoul National University, Seoul 08826, Korea; cameroncrazies@snu.ac.kr

<sup>5</sup> Interdisciplinary Program in Agricultural and Forest Meteorology, College of Agriculture and Life Sciences, Seoul National University, Seoul 08826, Korea

<sup>6</sup> National Center for Agro Meteorology, Seoul 08826, Korea

<sup>7</sup> Research Institute for Agriculture and Life Sciences, College of Agriculture and Life Sciences, Seoul National University, Seoul 08826, Korea

<sup>8</sup> Han River Basin Environmental Office, Hanam 12902, Korea; air3500@korea.kr

\* Correspondence: meehye@korea.ac.kr

**Abstract:** In order to identify the seasonal variability and source of carbonaceous aerosols in relation to haze occurrence, organic carbon (OC) and elemental carbon (EC) were continuously measured at the Taehwa Research Forest (TRF) near the Seoul metropolitan area from May 2013 to April 2014. For the entire experiment, the mean OC ( $5.1 \mu\text{gC}/\text{m}^3$ ) and EC ( $1.7 \mu\text{gC}/\text{m}^3$ ) concentrations of TRF were comparable to those of Seoul, with noticeably higher concentrations in winter and spring than in other seasons, and during haze days ( $6.6 \pm 3.2$  and  $2.1 \pm 1.0 \mu\text{gC}/\text{m}^3$ ) than during non-haze days ( $3.5 \pm 2.2$  and  $1.3 \pm 0.8 \mu\text{gC}/\text{m}^3$ ). The seasonal characteristics of OC and EC reveal the various sources of haze, including biomass combustion haze either transported for long distances or, in spring, from domestic regions, the greatest contribution of secondary organic carbon (SOC) in summer, and fossil fuel combustion in winter and fall. In addition, the seasonal OC/EC ratios between haze and non-haze days highlights that the increase in EC was more distinct than that of OC during haze episodes, thus suggesting that EC observed at a peri-urban forest site serves as a useful indicator for seasonally varying source types of haze aerosols in the study region.

**Keywords:** OC; EC; OC/EC ratio; seasonal haze; peri-urban forest site; Taehwa Research Forest



**Citation:** Ham, J.; Suh, I.; Lee, M.; Kim, H.; Kim, S. Elemental Carbon Observed at a Peri-Urban Forest Site near the Seoul Metropolitan Area as a Tracer of Seasonal Haze Occurrence. *Atmosphere* **2021**, *12*, 1627. <https://doi.org/10.3390/atmos12121627>

Academic Editor: Yunhua Chang

Received: 31 October 2021

Accepted: 3 December 2021

Published: 6 December 2021

**Publisher's Note:** MDPI stays neutral with regard to jurisdictional claims in published maps and institutional affiliations.



**Copyright:** © 2021 by the authors. Licensee MDPI, Basel, Switzerland. This article is an open access article distributed under the terms and conditions of the Creative Commons Attribution (CC BY) license (<https://creativecommons.org/licenses/by/4.0/>).

## 1. Introduction

Megacities in East Asia have experienced deteriorating air quality with rapid economic development, and the frequent occurrence of haze pollution has become a major public concern. Exposures to airborne fine particulate matter (PM) increases adverse effects on public health [1], particularly the respiratory and cardiovascular systems [2,3], causing premature deaths around the world. As a main cause for haze, PM<sub>2.5</sub> (PM smaller than 2.5 microns in mean aerodynamic diameter) is emitted directly or produced from various sources, such as fossil fuel combustion or biomass combustion such as forest fires and agricultural burning [4,5]. PM<sub>2.5</sub> also undergoes a long-range transformation.

Carbonaceous aerosols including organic carbon (OC) and elemental carbon (EC) constitute a significant fraction of PM<sub>2.5</sub> in the atmosphere. EC mainly originates from incomplete combustion of fossil fuels and biomasses, and affects the climate by exerting positive radiative forcing. Recent studies emphasized that exposure to EC has more adverse health effects than exposure to PM [6–11]. In comparison, OC is not only emitted from various combustion sources such as traffic exhaust and biomass burning, but also

forms through photochemical oxidation of gaseous precursors. It is therefore difficult to accurately distinguish between primary and secondary OC.

As the capital city of Korea, Seoul is one of the world's megacities and has recently suffered from haze pollution, especially during the cold months when continental outflows were most intensified. In Seoul, OC and EC concentrations were reported to be higher during winter and spring than in summer and fall [12]. This type of seasonality is observed in major cities in Korea, where the ratio of OC to EC varies due to the influence of local sources. For example, the OC/EC ratio is relatively low in Seoul due to the dominant contribution of vehicle emissions to carbonaceous aerosols. In comparison, open agricultural burning increases the contribution of OC to PM<sub>2.5</sub> mass concentration in other parts of Korea. In addition to the significant contribution of inorganic ions to PM<sub>2.5</sub> mass, carbonaceous aerosols also increase significantly during haze events. Therefore, it is important to investigate the characteristics of carbonaceous aerosols and identify their sources in urban areas, particularly during high PM<sub>2.5</sub> haze episodes.

In densely populated urban areas, green spaces have been expanded to mitigate air pollution and climate extremes such as heatwaves [13]. In terms of urban air quality, however, urban greening raises concerns about increases in O<sub>3</sub> and PM<sub>2.5</sub> owing to biogenic VOCs emitted from vegetation in NO<sub>x</sub> conditions [14]. In this context, the Teahwa Research Forest (TRF) has been established near the Seoul metropolitan area (SMA) to investigate the effects of mixed emissions of anthropogenic and natural sources, mainly from vehicles and vegetation, on air quality [15]. Previous studies conducted in this peri-urban site showed that O<sub>3</sub> increased with the increased level of biogenic emissions during the summer [16,17], while variations in primary species including reactive gases and particulate matters were similar to those of urban areas under the dominant influence of anthropogenic emission in other seasons [18]. During the KORUS-AQ (Korea US Air Quality Study) in 2016, the TRF served as one of the key ground measurement sites and the results demonstrated that TRF is suitable for investigating the role of vegetation in urban air quality and capturing pollution outflows from SMA, as well as long-distance transport [19].

In this study, we continuously determined OC and EC concentrations of PM<sub>2.5</sub>, along with reactive gases including O<sub>3</sub>, NO<sub>2</sub>, CO, and SO<sub>2</sub>, at the peri-urban TRF site for one year, and examined the seasonal variability and sources of carbonaceous aerosols with an emphasis on haze occurrence.

## 2. Experiment

### 2.1. Measurements

Measurements were conducted at Taehwa Research Forest (TRF, 37.18° N, 127.19° E), located about 45 km southeast of central Seoul (Figure 1). About a quarter of the Korean population resides in the Seoul metropolitan area (SMA), which includes Seoul and satellite cities around it. To the east of the TRF, a highway runs from north to south. The TRF site is equipped with a 41-m walk-in tower, which is located in the middle of the area (16 ha) afforested with coniferous Korean Pine trees (*Pinus koraiensis*) surrounded by a mixed forest with natural oak (476 ha) and coniferous trees (283 ha). Detailed information on the site can be found elsewhere [17,19,20].

The concentrations of OC and EC in PM<sub>2.5</sub> were measured with a semi-continuous OC/EC analyzer (Sunset Laboratory Inc., Tigard, OR, USA) from 7 May 2013 to 30 April 2014. OC and EC were determined every hour using the thermal optical transmittance (TOT) method, the NIOSH 5040 protocol, and the multistep temperature profile, through which the carbon fractions of OC and EC were quantified as CO<sub>2</sub> by a non-dispersive infrared (NDIR) detector. Thermal OC includes OC1, OC2, OC3, and OC4, evolving at 250 °C, 500 °C, 650 °C, and 850 °C, respectively. Pyrolyzed OC (OP) is defined as carbon evolved between the introduction of oxygen (O<sub>2</sub>: 2% and He: 98%) and the return of transmittance to its initial value [21]. After the full sequence of OC and EC analysis was completed, CH<sub>4</sub> (CH<sub>4</sub>: 5% and He: 95%) was injected to correct the precise amount of carbon. The quartz filter for sampling was replaced when the laser correction factor reached

0.88, and the filter blank was measured five times before resuming ambient measurements. The detection limits for OC and EC, determined by the three  $\sigma$  of the blank level, were  $0.27 \mu\text{gC}/\text{m}^3$  and  $0.01 \mu\text{gC}/\text{m}^3$ , respectively.

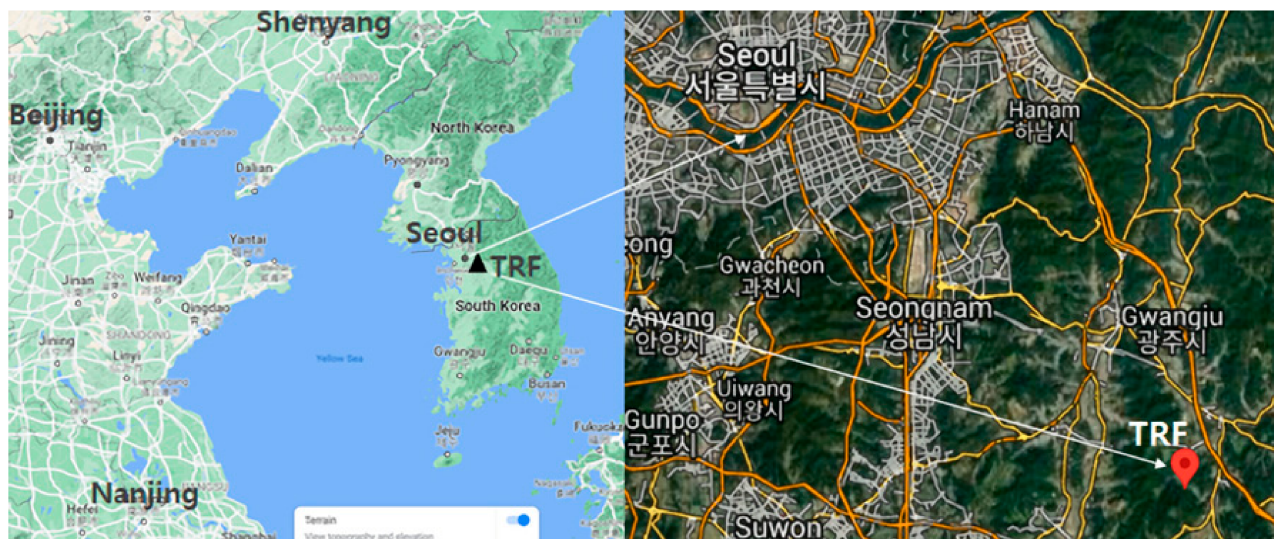


**Figure 1.** Measurement site of Taehwa Research Forest (TRF) near the Seoul metropolitan area (SMA), South Korea. Thick yellow lines indicate main highways (from Google Maps).

$\text{O}_3$ ,  $\text{NO}_x$ ,  $\text{CO}$ , and  $\text{SO}_2$  were measured every 1 min (49i, 42i, 48i, and 43C, Thermo Fisher Scientific, Waltham, MA, USA) and air was pumped from the inlet at a 4 m height on the 41 m tower. In addition, meteorological parameters, including temperature and relative humidity, were measured every 5 min (LSI meteorological instrument). These measurements were averaged over 1 h to be assimilated with the OC and EC measurements.

## 2.2. EC Tracer Method

The EC tracer method was applied to estimate the contribution of secondary organic carbon (SOC) to OC. It is one of the useful approaches for estimating the SOC concentration. Assuming that primary organic carbon (POC) originates from the same emission sources as EC, the difference between OC and POC is attributed to SOC [22,23]:

$$\text{POC} = (\text{OC}/\text{EC})_{\text{primary}} \times \text{EC} + b \quad (1)$$

$$\text{SOC} = \text{OC} - \text{POC} \quad (2)$$

where  $(\text{OC}/\text{EC})_{\text{primary}}$  indicates the primary OC to EC ratio, mostly emitted by combustion processes, and  $b$  is the POC produced from non-combustion processes. In this study,  $(\text{OC}/\text{EC})_{\text{primary}}$  was estimated from the lowest 5–20% subset of the OC and EC data [24,25].

## 2.3. Air Mass Back Trajectory Analysis

The backward trajectory of the air mass reaching the sampling site at an altitude of 500 m was calculated for 48 h using the National Oceanic and Atmospheric Administration (NOAA) HYSPLIT-4 model with Global Data Assimilation System (GDAS) data produced by the National Center for Environmental Prediction. More details about the HYSPLIT model can be found at <http://www.arl.noaa.gov/ready/open/hysplit4.html> (NOAA Air Resources Laboratory), accessed on 1 October 2021. The model was run four times a day at 04:00, 10:00, 16:00, and 22:00 UTC (12:00, 18:00, 00:00, and 06:00 local time).

Concentration-weighted trajectory (CWT) analysis is a method for identifying potential source regions based on the HYSPLIT model. In each grid cell, a weighted concentration

of a species is obtained by averaging measured concentrations associated with trajectories crossing the grid cell as follows [26]:

$$C_{(i,j)} = \frac{1}{\sum_{l=1}^M \tau_{ijl}} \sum_{l=1}^M C_l \tau_{ijl} \quad (3)$$

where  $i$  and  $j$  are the indices of grid,  $l$  is the index of trajectory,  $M$  is the total number of trajectories used in analysis,  $C_l$  is the species concentration measured on the arrival of trajectory  $l$ , and  $\tau_{ijl}$  is the residence time of trajectory  $l$  in the grid cell  $(i, j)$ . The CWT model was run using the R-based openair package [27].

### 3. Results and Discussion

#### 3.1. High OC and EC Concentration in Cold Months

For the entire experiment period, mean and maximum OC, EC, and TC concentrations were  $5.1 \pm 3.2 \mu\text{gC}/\text{m}^3$  and  $1.7 \pm 1.0 \mu\text{gC}/\text{m}^3$ ,  $6.8 \pm 3.9 \mu\text{gC}/\text{m}^3$  and  $22.7 \mu\text{gC}/\text{m}^3$ ,  $8.0 \mu\text{gC}/\text{m}^3$ , and  $27.3 \mu\text{gC}/\text{m}^3$ , respectively. These average OC and EC concentrations were higher than those observed in Jeju ( $2.9 \mu\text{gC}/\text{m}^3$  and  $0.8 \mu\text{gC}/\text{m}^3$ ) [28], the background of Northeast Asia, and comparable to those observed in Seoul ( $5.9 \mu\text{gC}/\text{m}^3$  and  $1.2 \mu\text{gC}/\text{m}^3$ ) [29] (Table 1). Note that the TRF is a peri-urban forest site due to its proximity to the SMA (Figure 1). However, these three sites showed similar seasonal variation with higher concentrations in cold months (November to March) than in warm months (April to October). The monthly variations of these two species are presented with reactive gases and meteorological parameters in Figure 2. It is evident that OC and EC were inversely correlated with  $\text{O}_3$ , which is usually higher from May to June. During warm months, the primary gases such as CO and  $\text{SO}_2$  were usually at their minimum levels. This is typical seasonality of atmospheric chemical constituents observed in the northeast Asia region. In Beijing, with much higher OC and EC concentrations than the TRF, the concentrations of these gases were also higher in the cold season than the warm season [30] (Table 1). These results suggest that the high OC and EC concentrations of the cold months reflect the regional characteristics that is highly susceptible to meteorological conditions.

**Table 1.** Comparison of average concentration of OC, EC, and  $\text{PM}_{2.5}$  at several sites in northeast Asia.

Site (Type)	$\text{PM}_{2.5}$ ( $\mu\text{gC}/\text{m}^3$ )	OC ( $\mu\text{gC}/\text{m}^3$ )	EC ( $\mu\text{gC}/\text{m}^3$ )
This study, TRF (peri-urban)	-	5.1	1.7
Seoul, South Korea (urban)	30.6	5.9	1.2
Jeju, South Korea (background)	18.6	2.9	0.8
Beijing, China (urban)	93.8	14.0	4.1

For in-depth discussion, the measurements were divided into five seasons according to synoptic meteorological conditions (Table 2). In the study region, the monsoon system develops in winter and summer. Winter is characterized by strong northerly winds from the continent during December to February. The summer monsoon is accompanied with heavy rains from the end of June to September, during which all air pollutants remained at the minimum levels. Due to heavy rains, the measurements were halted from July to the middle of August in this study. Before the monsoon season began, the air is highly stagnant, leading to an increase in  $\text{O}_3$  mixing ratio in May to June and  $\text{PM}_{2.5}$  mass concentration in October to November, which were classified as early summer and fall, respectively. In the spring from March to April, the frontal system develops and expedites the transport of continental outflows such as Asian dust.

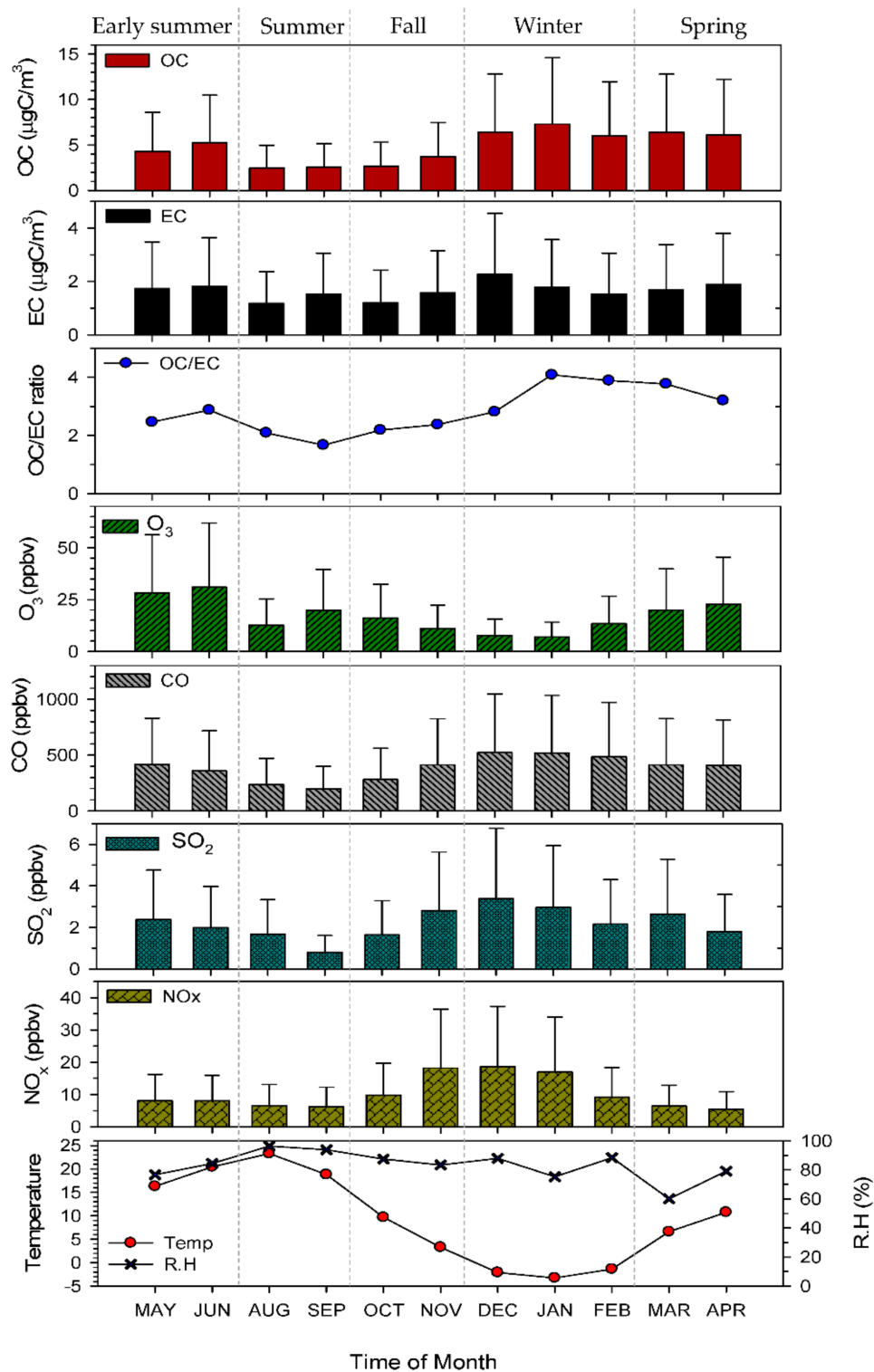


Figure 2. Variations in monthly mean OC, EC, OC/EC ratio, O<sub>3</sub>, CO, SO<sub>2</sub>, NO<sub>x</sub>, and metrological parameters.

**Table 2.** Seasonal characteristics of carbonaceous aerosols, reactive gases, and metrological factors observed in the Taehwa Research Forest (TRF) from May 2013 to April 2014. The period was divided into haze days and non-haze days.

Title	Total			Early Summer (May–June)			Summer (August–September)			Fall (October–November)			Winter (December–February)			Spring (March–April)		
	All	Haze	Non-Haze	All	Haze	Non-Haze	All	Haze	Non-Haze	All	Haze	Non-Haze	All	Haze	Non-Haze	All	Haze	Non-Haze
Frequency of days	280	136	144	49	41	16	41	5	36	52	15	37	89	48	41	49	35	14
OC ( $\mu\text{gC}/\text{m}^3$ )	5.1	6.6	3.5	4.9	5.5	3.4	2.5	3.3	2.4	3.3	4.6	2.7	6.7	7.9	4.9	6.2	6.9	4.1
EC ( $\mu\text{gC}/\text{m}^3$ )	1.7	2.1	1.3	1.8	1.9	1.5	1.4	1.3	1.4	1.4	2.0	1.1	1.9	2.3	1.4	1.8	2.1	1.0
OC/EC	3.15	3.34	2.95	2.84	3.05	2.37	1.98	2.56	1.90	2.46	2.24	2.57	3.82	3.74	3.93	3.84	3.63	4.44
O <sub>3</sub> (ppb)	16.8	18.3	15.1	29.9	32.2	25.2	16.3	19.9	15.7	13.1	11.4	14.	8.9	8.2	9.8	21.8	22.6	19.5
CO (ppb)	407	480	323	379	402	332	217	268	209	362	504	287	511	581	424	410	430	357
SO <sub>2</sub> (ppb)	2.3	3.0	1.6	2.1	2.3	1.7	1.2	1.6	1.2	2.4	3.2	1.9	2.9	3.8	1.8	2.1	2.5	1.0
NO <sub>x</sub> (ppb)	10.6	11.9	9.0	7.5	7.5	7.4	5.6	6.6	5.5	14.4	21.3	10.9	15.1	17.1	12.4	5.5	5.9	4.4
Temp. (°C)	8.0	7.7	8.3	18.9	18.9	18.4	21.4	22.3	21.2	4.8	5.1	4.7	−2.4	−2.0	−2.9	9.2	9.9	7.1
RH (%)	83.4	82.9	84.0	82.3	79.5	87.9	95.3	95.7	95.3	84.3	89.0	81.6	83.0	85.6	77.3	76.2	77.4	73.8

OC and EC concentrations were much higher, with higher CO and SO<sub>2</sub> mixing ratios, in winter and spring than in other seasons. During the experimental period from 2013 to 2014, severe winter haze events occurred frequently in northern China as well as the SMA. In the TRF, the number of haze days was 48, 35, and 41, in winter, spring, and early summer, respectively (Table 2). In Korea, haze is defined by the Korea Meteorological Administration (KMA) as a meteorological phenomenon when relative humidity is below 70% with visibility between 1 and 10 km. Overall, the average OC and EC concentrations were significantly higher on haze days ( $6.6 \pm 3.2$  and  $2.1 \pm 1.0 \mu\text{gC}/\text{m}^3$ ) than on non-haze days ( $3.5 \pm 2.2$  and  $1.3 \pm 0.8 \mu\text{gC}/\text{m}^3$ ), suggesting OC and EC as major constituents of haze aerosol. Table 2 compares the mean concentrations of OC and EC and the OC/EC ratio for haze and non-haze days in five seasons, along with O<sub>3</sub>, CO, SO<sub>2</sub>, NO<sub>x</sub>, and meteorological parameters such as RH and temperature.

### 3.2. Seasonal Variability in OC and EC

In all seasons, OC and EC concentrations increased noticeably during haze periods compared to non-haze periods, except for EC in summer (Table 2). As in the haze period, OC concentrations in the non-haze period were also much higher in winter and spring than in other seasons. In contrast, the EC concentration in non-haze periods was high during the two summer seasons and low in fall and spring. As a result, the increase of OC on haze days relative to non-haze days remained nearly constant throughout the season, whereas the EC enhancement varied season to season, with the highest enhancement in spring and the lowest in early summer. Summer, especially, was characterized by the greatest impact of local emissions with limited continental outflows. In urban areas, EC or black carbon (BC) can serve as a surrogate for emissions of PM mass concentrations due to its short lifetime and few natural or secondary sources compared to OC [31]. A recent study also demonstrates that in Seoul during the summer, BC was mostly fresh soot particles, a by-product of fossil fuel combustion from local sources [32].

At the peri-urban TRF site, the OC/EC ratio was higher in non-haze periods than in haze periods from fall to spring, even though these ratios were evidently high in spring and winter. In the two summer seasons, on the other hand, the OC/EC ratio was higher during haze events. This result reveals the role of secondary organic carbon (SOC) in increasing OC concentration. Overall, the OC/EC ratio of the five seasons was the highest in winter and spring, with increased OC and EC concentrations (Figure 2). In previous studies, high OC/EC ratios have been regarded as the effect of secondary OC. Therefore, the seasonal contribution of SOC to OC was estimated.

### 3.3. High SOC to OC Ratio in Warm Months

In the present study, the SOC concentration was estimated from the measured OC concentrations using the EC tracer method; the results are summarized in Table 3. While the OC concentration was higher in winter and spring, while the estimated SOC concentration and its fraction compared to OC was the highest in early summer, suggesting that SOC was not a main cause of high OC/EC ratios in colder months. Moreover, the previous studies showed that in the TRF, BOVC concentrations were the highest in June under high temperatures and sunlight [17]. Thus, warmer months were more favorable to the formation of SOC. In early summer, the diurnal variation of the SOC/OC ratio showed a clear peak in the afternoon, which was in accordance with the O<sub>3</sub> maximum. In contrast, EC reached a maximum in the early morning, which was concurrent with the CO maximum. Along with primary OC, these two species were thought to be emitted from vehicles on the highway east of the TRF. Therefore, it is likely that SOC played a significant role in increasing OC and the OC /EC ratio only in early summer.

**Table 3.** For each season,  $(OC/EC)_{\text{primary}}$ ,  $b$ , and coefficient of determination ( $r^2$ ) in Equations (1) and (2) in the text, and the average concentrations of SOC and the ratio of SOC to OC.

Period	$(OC/EC)_{\text{primary}}$	$b$	$r^2$	SOC ( $\mu\text{gC}/\text{m}^3$ )	SOC/OC (%)
Early summer (May–Jun)	0.83	0.36	0.61	3.37	70.8
Fall (Oct–Nov)	0.80	0.20	0.55	1.92	60.1
Winter (Dec–Feb)	1.90	0.12	0.83	3.05	45.9
Spring (Mar–Apr)	1.66	0.38	0.84	3.18	51.2

If the estimated  $(OC/EC)_{\text{primary}}$  represents the primary emissions from local combustion sources [33–35], its seasonal variability would be insignificant. As listed in Table 3, however, it is more than two times higher in winter and spring than in early summer and fall. The background OC/EC ratio was enhanced as well, and the correlation was the best between OC and EC and the CO and SO<sub>2</sub> mixing ratios. These seasonal characteristics are typical in northeast Asia, where the influence of long-range transport is dominant in the cold season [23,24]. It has been also recognized that the estimated POC includes OC other than freshly emitted POC, such as OC from the oxidation of the evaporated POC and long-distance transport [36]. To see if the OC/EC ratio is related with the seasonal characteristics of air masses at the TRF, the degree of photochemical aging was evaluated for the five seasons.

### 3.4. Chemical Characteristics of TRF Air Masses

The ratios of reactive gases such as O<sub>3</sub>/NO<sub>x</sub> and CO/NO<sub>x</sub> are suggested to be useful indicator for proximity to emission sources and degree of photochemical processing [37,38], where these ratios were observed to be increased as urban plumes are transported from the sources regions. In Figure 3, the hourly measurements of TRF are presented by season. In this study, the photochemical evolution of air masses was seasonally distinguished. The lowest O<sub>3</sub>/NO<sub>x</sub> ratios of winter air masses correspond to those of “urban”, which progressively leads to spring air masses. In summer, air masses were aged with characteristics of near-outflow air. The high OC and EC were associated with air masses of cold months other than summer, when the SOC/OC ratios were evidently high. In general, Northeast Asia is under influence of aged marine air mass in summer, while relatively less aged air mass was observed in the winter when continental outflow is intensified.

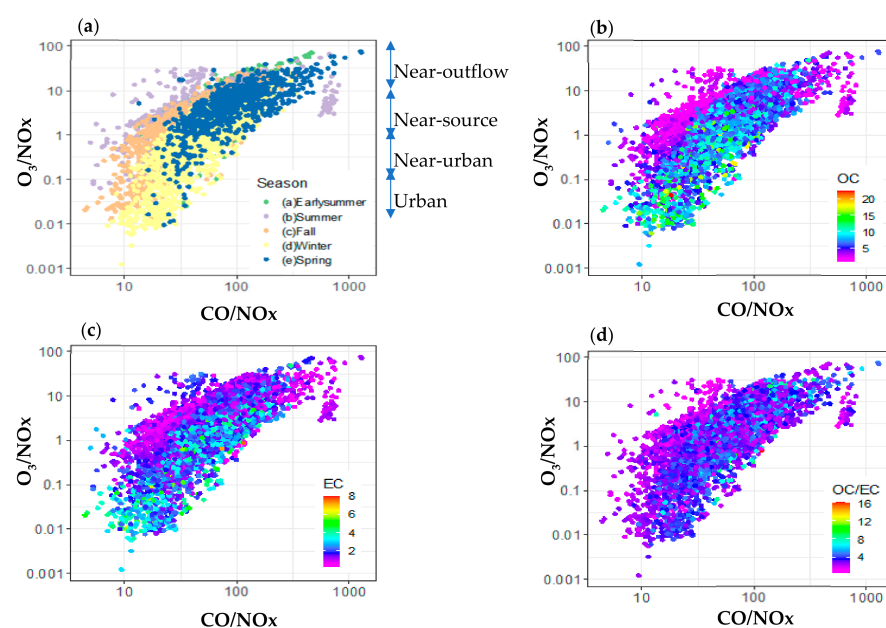


**Figure 3.** In the coordinate of O<sub>3</sub>/NO<sub>x</sub> ratio versus CO/NO<sub>x</sub> ratio, all hourly measurements color-coded by (a) season, (b) OC concentrations, (c) EC concentration, and (d) OC/EC ratios.

The CO/NO<sub>x</sub> ratios were higher in cold months than those of warm months. The previous studies reported that CO concentration was elevated with carbonaceous aerosol in Asian continental outflows and demonstrated that Chinese plumes were identified by higher CO/NO<sub>x</sub> ratios [38–41]. Accordingly, our results confirm that the photochemical characteristics of TFR was largely affected by synoptic meteorological condition and thereby the source of carbonaceous aerosol. In the cold months, the high OC/EC ratios was thought to be the influence of the transported sources. In the next section, the source of OC and EC was analyzed using air mass trajectories.

### 3.5. Source Signatures of OC and EC

For EC and OC, CWT analysis was conducted for 48 h in R Open air package and the potential source areas were identified (Figure 4). The result highlights the north eastern and eastern China as source regions for the high OC and EC observed in TRF, particularly in winter. As mentioned in earlier section, PM<sub>2.5</sub> haze events occurred frequently during the experiment period, when OC and EC concentration were significantly elevated. It is consistent with what have been observed in China, even though secondary inorganic constituents were more remarkably elevated than carbonaceous aerosols during severe wintertime pollution episodes [42–44]. Similarly in South Korea, the increase in nitrate was most pronounced in high PM<sub>2.5</sub> episodes during cold months [45]. The relative increase in inorganic and carbonaceous aerosol is highly dependent on synoptic weather conditions that determine the type of sources such as fossil or biomass and the aging processes of fine aerosol during the transport.

In this section, the detailed source characteristics were examined using CWT analysis for all measured species including reactive gases. Potential sources of OC and EC were compared with all measurements for the seasonal haze occurrences (Figure 4). For both OC and EC, the northern China plain and northeastern China are distinguished as sources contributing to high OC and EC, which were almost identical to those for winter haze. While high OC and EC were closely linked in their sources during the winter and fall haze, they were decoupled during the spring haze. Interestingly, the great contributions of carbonaceous aerosols were found in the western coastal regions of the Korean peninsula and in the eastern coast of China during the spring, and over the Yellow Sea and near TRF during the fall. In particular, high concentrations of both OC and EC are evident in the southwestern part of the Korean Peninsula in spring, suggesting the contribution of agricultural combustion. In the early summer, high concentrations of OC and EC were dominated by local sources. Results from these TRF confirm the crucial contribution of increased OC and EC during haze generation. In addition, the major sources of OC and EC are different from season to season.

To elucidate the seasonal differences in OC and EC sources, their relation to reactive gases and meteorological parameters were compared (Figure 5). The seasonal mean CO and temperature were inversely correlated, while ozone proportionally increased with temperature. It is a typical seasonality observed in the study region. As a good tracer for combustion processes, CO was also reported to indicate the influence of transport from Asian continent (e.g., Jordan et al., 2020) [45]. Accordingly, CO mixing ratio was higher during the winter than the other seasons. EC was correlated very well with CO and SO<sub>2</sub>, suggesting the dominant contribution from fossil fuel sources to carbonaceous aerosol throughout the year. In comparison, the correlation of OC with CO was not as good as that of EC. Particularly, OC concentration was low relative to CO in fall, when NO<sub>x</sub> mixing ratio was the highest. Figure 4 displays that during the fall, high OC and EC concentrations were confined to the Yellow Sea and near the TRF, reflecting synoptic-scale stagnation favorable for haze development. The comparison of measured species between haze days and non-haze days highlights the greatest enhancement of CO as well as NO<sub>x</sub> in the fall (Table 4), suggesting the increased contribution of local emissions from vehicles and transported sources to fall haze under stagnant conditions. Consequently, this indicates the role of synoptic conditions and local influence in haze development.

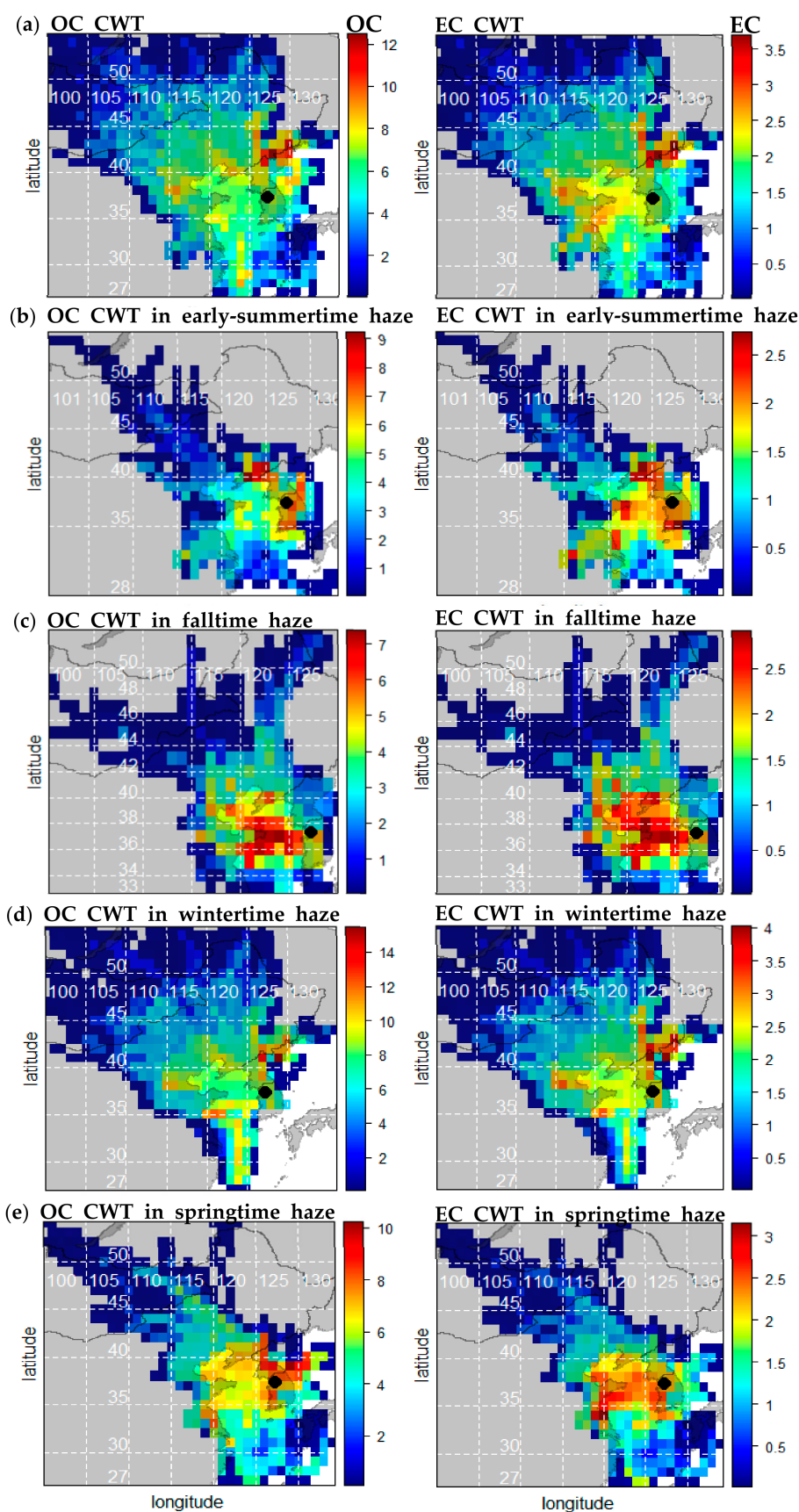


**Figure 4.** The CWT analysis results for OC and EC mean concentrations ( $\mu\text{gC}/\text{m}^3$ ) during the (a) entire measurement period, (b) early summer haze, (c) fall haze, (d) winter haze, and (e) spring haze.

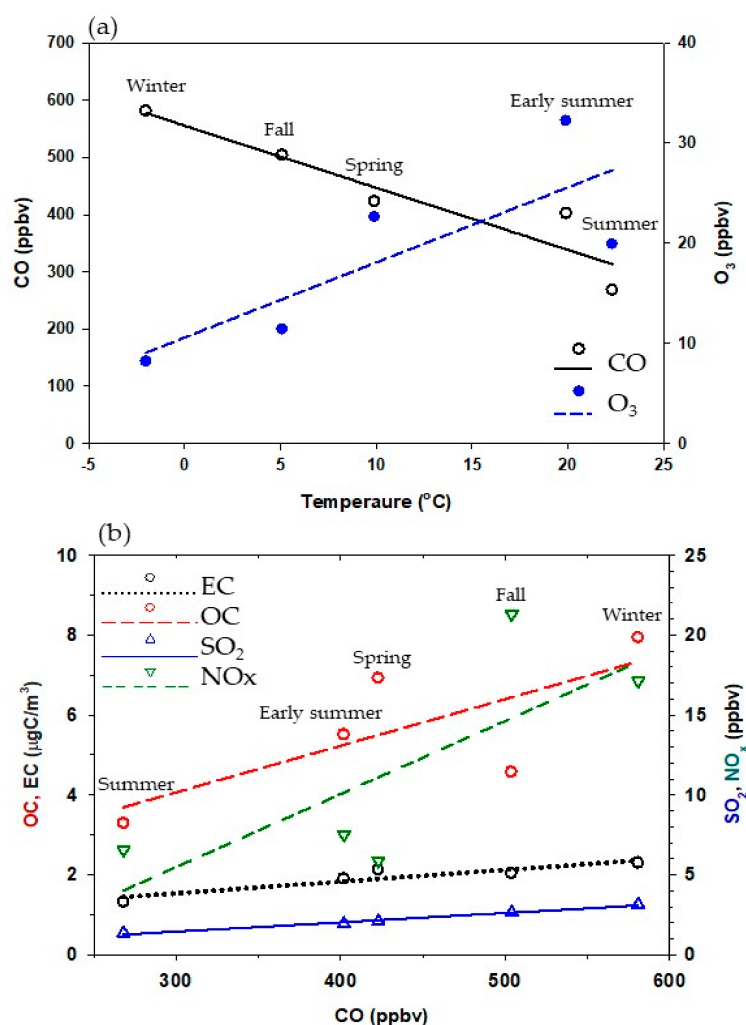


**Figure 5.** Correlations of seasonal mean concentrations of (a) CO and O<sub>3</sub> versus temperature and (b) OC, EC, SO<sub>2</sub> and NO<sub>x</sub> versus CO mixing ratio during the haze episodes (Table 2). The line represents the linear regression fit.

**Table 4.** The ratios of the haze to non-haze days for measured species including OC, EC, CO, SO<sub>2</sub>, NO<sub>x</sub>, relative humidity (RH), temperature, and OC/EC ratio.

Season	OC	EC	OC/EC	CO	SO <sub>2</sub>	NO <sub>x</sub>	RH	Temp.
Early Summer	1.62	1.24	1.29	1.21	1.35	1.02	0.90	1.03
Fall	1.69	1.78	0.87	1.75	1.63	1.95	1.09	1.08
Winter	1.70	1.68	0.95	1.37	2.15	1.38	1.11	1.49
Spring	1.66	2.15	0.82	1.20	2.53	1.34	1.05	1.39

On the other hand, OC was highly elevated with the minimum level of NO<sub>x</sub> in the spring, when the trajectory of high OC was decoupled from that of EC (Figures 4 and 5). The highest OC was associated with the trajectories passing through northeastern China and eastern Russia under northerly and easterly winds (Figure 4). In this region, fire activities have sharply increased in spring due to agricultural burning to prepare fields (<https://worldview.earthdata.nasa.gov/>), accessed on 1 October 2021. Similarly in the western region of Korean peninsula (Figure 1), farmland is usually burned in spring, which is also distinguished as source areas for carbonaceous aerosols, especially EC in Figure 4. Therefore, our results reveal the contribution of biomass combustion to OC and consequently the occurrence of haze in spring. In the present study, the seasonal characteristics of OC and EC reveal the various sources of haze such as biomass combustion transported

for a long distance and from domestic regions in spring, the greatest contribution of SOC in summer, and fossil fuel combustion in winter and fall.

### 3.6. EC as a Tracer for Haze

For all seasons, the concentrations of carbonaceous aerosols and precursor gases were higher on haze days than on non-haze days (Table 4). It was evident in this study that OC was highly elevated on haze days, but interestingly, the relative increase in OC on haze to non-haze days was almost constant throughout the year. In comparison, the enhancement of EC on haze days varied from season to season, with the greatest in spring (2.15) and the least in early summer (1.24). The different enhancement of OC and EC is primarily associated with the contribution of SOC to OC. Note that the ratio of SOC/OC was greatest in the early summer (Table 3). It is also noteworthy that concentrations of carbonaceous aerosols and precursor gases exhibited a negligible difference between haze and non-haze days during the summer, indicating the dominant impact of local emissions on haze occurrence (Table 4).

In addition to SOC, the relative increase in carbonaceous aerosols on haze days compared to non-haze days was possibly affected by their source types. As discussed above, biomass combustion played a significant role in increasing OC in spring, while the impact of vehicle emissions was revealed by relatively large increase in NO<sub>x</sub> and a low OC/EC ratio on haze days in the fall. The difference in OC/EC ratios between haze and non-haze days was insignificant in winter (0.95). In comparison, this ratio was 1.29 in early summer and lower than 1 in spring (0.82) and fall (0.87). This was mainly due to the distinct increase in EC during haze episodes compared to non-haze episodes. OC and EC observed in the TRF showed different characteristics when haze occurred, mainly due to seasonally varying sources and the secondary formation of OC during the transport of air masses and. In contrast, the intrinsic properties of EC are likely to be preserved after being emitted from sources. Therefore, EC is proposed as a useful indicator for seasonally varying source types of haze aerosols in the study region.

## 4. Conclusions

From May 2013 to April 2014, the OC and EC concentrations of PM<sub>2.5</sub> were continuously measured every hour in the peri-urban Taehwa Research Forest (TRF) site near the Seoul metropolitan area. The mean concentrations of OC and EC were  $5.1 \pm 3.2 \mu\text{gC}/\text{m}^3$  and  $1.7 \pm 1.0 \mu\text{gC}/\text{m}^3$ , respectively, which were comparable to those observed in Seoul. In particular, these two species showed a clear seasonal pattern, being lower in the warm months and higher in the cold months. The ratio of OC to EC was also noticeably high in spring and winter. In particular, the seasonal OC and EC concentrations were significantly higher on haze days ( $6.6 \pm 3.2$  and  $2.1 \pm 1.0 \mu\text{gC}/\text{m}^3$ ) than non-haze days ( $3.5 \pm 2.2$  and  $1.3 \pm 0.8 \mu\text{gC}/\text{m}^3$ ), suggesting OC and EC as major constituents of haze aerosol.

The increase of OC on haze days relative to non-haze days remained nearly constant throughout the season, whereas the EC enhancement varied season to season, with the highest in spring and the lowest in early summer. As a result, the OC/EC ratio was lower in haze periods than in non-haze periods from fall to spring (the two summer seasons). This was mainly due to the contribution of SOC to OC. Indeed, the contribution of estimated secondary OC (SOC) to OC was the highest in early summer. In addition, the high OC/EC ratios were found in the near-urban regime that was distinguished by low O<sub>3</sub>/NO<sub>x</sub> and CO/NO<sub>x</sub> ratios.

The results of the CWT analysis reveal the potential sources of high OC and EC during seasonally occurring haze events, including biomass combustion associated with agricultural activities in spring, SOC and EC from local emissions in summer, and fossil fuel combustion in winter and fall. The one-year measurements of OC and EC at the peri-urban TRF site near the Seoul metropolitan area highlights that the seasonal variation in EC was more distinct than OC during haze episodes, thereby suggesting that EC is a useful indicator for seasonal haze occurrence in the study region.

**Author Contributions:** All authors performed the experiments, and data collection, and analysis. All authors have read and agreed to the published version of the manuscript.

**Funding:** This study was supported by the Korea Institute of Science and Technology (KIST) through grant 2E31290-21-P009. A special thank is given to the Institute of Environmental Research (NIER) for providing the research facilities and supporting the measurements.

**Institutional Review Board Statement:** Not applicable.

**Informed Consent Statement:** Not applicable.

**Data Availability:** Data used in this study will be available upon request to the corresponding author.

**Conflicts of Interest:** The authors declare no conflict of interest.

## References

1. Hassan, A.; Ilyas, S.Z.; Agathopoulos, S.; Hussain, S.M.; Jalil, A.; Ahmed, S.; Baqir, Y. Evaluation of adverse effects of particulate matter on human life. *Heliyon* **2021**, *7*, 2405–8440. [[CrossRef](#)] [[PubMed](#)]
2. Raaschou-Nielsen, O.; Andersen, Z.J.; Beelen, R.; Samoli, E.; Stafoggia, M.; Weinmayr, G.; Hoffmann, B.; Fischer, P.; Nieuwenhuijsen, M.J.; Brunekreef, B.; et al. Air pollution and lung cancer incidence in 17 European cohorts: Prospective analyses from the European Study of Cohorts for Air Pollution Effects (ESCAPE). *Lancet Oncol.* **2013**, *14*, 813–822. [[CrossRef](#)]
3. Cohen, A.J.; Anderson, H.R.; Ostro, B.; Pandey, K.D.; Krzyzanowski, M.; Künzli, N.; Gutschmidt, K.; Pope, A.; Romieu, I.; Samet, J.M.; et al. The Global Burden of Disease Due to Outdoor Air Pollution. *J. Toxicol. Environ. Health Part A.* **2005**, *68*, 1528–7394. [[CrossRef](#)] [[PubMed](#)]
4. Thepnuan, D.; Chantara, S.; Lee, C.T.; Lin, N.H.; Tsai, Y.I. Molecular markers for biomass burning associated with the characterization of PM<sub>2.5</sub> and component sources during dry season haze episodes in Upper South East Asia. *Sci. Total Environ.* **2019**, *658*, 708–722. [[CrossRef](#)] [[PubMed](#)]
5. Lim, H.-J.; Turpin, B.J. Origins of Primary and Secondary Organic Aerosol in Atlanta: Results of Time-Resolved Measurements during the Atlanta Supersite Experiment. *Environ. Sci. Technol.* **2002**, *36*, 4489–4496. [[CrossRef](#)]
6. Song, S.-K.; Choi, Y.-N.; Choi, Y.; Flynn, J.; Sadeghi, B. Characteristics of aerosol chemical components and their impacts on direct radiative forcing at urban and suburban locations in Southeast Texas. *Atmos. Environ.* **2021**, *246*, 1352–2310. [[CrossRef](#)]
7. Janssen, N.A.H.; Hoek, G.; Simic-Lawson, M.; Fischer, P.; van Bree, L.; ten Brink, H.; Keuken, M.; Atkinson, R.W.; Anderson, H.R.; Brunekreef, B.; et al. Black Carbon as an Additional Indicator of the Adverse Health Effects of Airborne Particles Compared with PM<sub>10</sub> and PM<sub>2.5</sub>. *Environ. Health Perspect.* **2011**, *119*, 1691–1699. [[CrossRef](#)]
8. Boniardi, L.; Dons, E.; Longhi, F.; Scuffi, C.; Campo, L.; Poppel, M.V.; Panis, L.I.; Fustinoni, S. Personal exposure to equivalent black carbon in children in Milan, Italy: Time-activity patterns and predictors by season. *Environ. Pollut.* **2021**, *274*, 116530. [[CrossRef](#)] [[PubMed](#)]
9. Pani, S.K.; Wang, S.-H.; Lin, N.-H.; Chantara, S.; Lee, C.-T.; Thepnuan, D. Black carbon over an urban atmosphere in northern peninsular Southeast Asia: Characteristics, source apportionment, and associated health risks. *Environ. Pollut.* **2020**, *259*, 113871. [[CrossRef](#)] [[PubMed](#)]
10. Lin, W.; Dai, J.; Liu, R.; Zhai, Y.; Yue, D.; Hu, Q. Integrated assessment of health risk and climate effects of black carbon in the Pearl River Delta region, China. *Environ. Res.* **2019**, *176*, 108522. [[CrossRef](#)]
11. Li, Y.; Henze, D.K.; Jack, D.; Henderson, B.H.; Kinney, P.L. Assessing public health burden associated with exposure to ambient black carbon in the United States. *Sci. Total Environ.* **2016**, *539*, 515–525. [[CrossRef](#)] [[PubMed](#)]
12. Park, J.S.; Song, I.H.; Park, S.M.; Shin, H.J. The Characteristics and Seasonal Variations of OC and EC for PM<sub>2.5</sub> in Seoul Metropolitan Area in 2014. *J. Environ. Impact Assess.* **2015**, *24*, 578–592. [[CrossRef](#)]
13. Baumgardner, D.; Varela, S.; Escobedo, F.J.; Chacalo, A.; Ochoa, C. The role of a peri-urban forest on air quality improvement in the Mexico City megalopolis. *Environ. Pollut.* **2012**, *163*, 174–183. [[CrossRef](#)] [[PubMed](#)]
14. Gu, S.; Alex, G.; Celia, F. Effects of Anthropogenic and Biogenic Volatile Organic Compounds on Los Angeles Air Quality. *Environ. Sci. Technol.* **2021**, *55*, 12191–12201. [[CrossRef](#)] [[PubMed](#)]
15. Kim, S.-Y.; Jiang, X.; Lee, M.; Turnipseed, A.; Guenther, A.; Kim, J.-C.; Lee, S.-J.; Kim, S. Impact of biogenic volatile organic compounds on ozone production at the Taehwa Research Forest near Seoul, South Korea. *Atmos. Environ.* **2013**, *70*, 447–453. [[CrossRef](#)]
16. Ham, J.; Lee, M.; Kim, H.S.; Park, H.; Cho, G.; Park, J. Variation of OC and EC in PM<sub>2.5</sub> at Mt. Taehwa. *J. Korean Soc. Atmos. Environ.* **2016**, *32*, 21–31. [[CrossRef](#)]
17. Kim, H.; Lee, M.; Kim, S.; Guenther, A.; Park, J.; Cho, G.; Kim, H. Measurements of Isoprene and Monoterpenes at Mt. Taehwa and Estimation of Their Emissions. *Korean J. Agric. For. Meteorol.* **2015**, *17*, 217–226. [[CrossRef](#)]
18. Gil, J.; Lee, M.; Han, J.; Kim, S.; Guenther, A.; Kim, H.; Kim, S.; Park, H. Peroxyacetyl Nitrate and Ozone Enhancement at Taehwa Research Forest under the Influence of Seoul Metropolitan Area. *Aerosol Air Qual. Res.* **2018**, *18*, 2262–2273. [[CrossRef](#)]

19. Lim, S.; Lee, M.; Czimczik, C.I.; Joo, T.; Holden, S.; Mouteva, G.; Santos, G.M.; Xu, X.; Walker, J.; Kim, S.; et al. Source signatures from combined isotopic analyses of PM<sub>2.5</sub> carbonaceous and nitrogen aerosols at the peri-urban Taehwa Research Forest, South Korea in summer and fall. *Sci. Total Environ.* **2019**, *655*, 1505–1514. [[CrossRef](#)] [[PubMed](#)]
20. Sullivan, J.T.; McGee, T.J.; Stauffer, R.M.; Thompson, A.M.; Weinheimer, A.; Knote, C.; Janz, S.; Wisthaler, A.; Long, R.; Szykman, J.; et al. Taehwa Research Forest: A receptor site for severe domestic pollution events in Korea during 2016. *Atmos. Chem. Phys.* **2019**, *19*, 5051–5067. [[CrossRef](#)]
21. Chow, J.C.; Watson, J.G.; Pritchett, L.C.; Pierson, W.R.; Frazier, C.A.; Purcell, R.G. The dri thermal/optical reflectance carbon analysis system: Description, evaluation and applications in U.S. Air quality studies. *Atmos. Environ. Part A. Gen. Top.* **1993**, *27*, 1185–1201. [[CrossRef](#)]
22. Turpin, B.J.; Huntzicker, J.J. Identification of secondary organic aerosol episodes and quantitation of primary and secondary organic aerosol concentrations during SCAQS. *Atmos. Environ.* **1995**, *29*, 3527–3544. [[CrossRef](#)]
23. Cabada, J.C.; Pandis, S.N.; Subramanian, R.; Robinson, A.L.; Polidori, A.; Turpin, B. Estimating the Secondary Organic Aerosol Contribution to PM<sub>2.5</sub> Using the EC Tracer Method Special Issue of Aerosol Science and Technology on Findings from the Fine Particulate Matter Supersites Program. *Aerosol Sci. Technol.* **2004**, *38*, 140–155. [[CrossRef](#)]
24. Polidori, A.; Turpin, B.J.; Lim, H.-J.; Cabada, J.C.; Subramanian, R.; Pandis, S.N.; Robinson, A.L. Local and Regional Secondary Organic Aerosol: Insights from a Year of Semi-Continuous Carbon Measurements at Pittsburgh. *Aerosol Sci. Technol.* **2006**, *40*, 861–872. [[CrossRef](#)]
25. Yuan, Z.B.; Yu, J.Z.; Lau, A.K.H.; Louie, P.K.K.; Fung, J.C.H. Application of positive matrix factorization in estimating aerosol secondary organic carbon in Hong Kong and its relationship with secondary sulfate. *Atmos. Chem. Phys.* **2006**, *6*, 25–34. [[CrossRef](#)]
26. Hsu, Y.; Holsen, T.M.; Hopke, P.K. Comparison of hybrid receptor models to locate PCB sources in Chicago. *Atmos. Environ.* **2003**, *37*, 545–562. [[CrossRef](#)]
27. Carslaw, D.C.; Ropkins, K. openair—An R package for air quality data analysis. *Environ. Model. Softw.* **2012**, *27–28*, 52–61. [[CrossRef](#)]
28. Kim, J.A.; Lim, S.; Shang, X.; Lee, M.; Kang, K.S.; Ghim, Y.S. Characteristics of PM<sub>2.5</sub> Chemical Composition and High-concentration Episodes Observed in Jeju from 2013 to 2016. *J. Korean Soc. Atmos. Environ.* **2020**, *36*, 388–403. [[CrossRef](#)]
29. Kim, Y.; Yi, S.-M.; Heo, J. Fifteen-year trends in carbon species and PM<sub>2.5</sub> in Seoul, South Korea (2003–2017). *Chemosphere* **2020**, *261*, 127750. [[CrossRef](#)] [[PubMed](#)]
30. Ji, D.; Zhang, J.; He, J.; Wang, X.; Pang, B.; Liu, Z.; Wang, L.; Wang, Y. Characteristics of atmospheric organic and elemental carbon aerosols in urban Beijing, China. *Atmos. Environ.* **2016**, *125*, 293–306. [[CrossRef](#)]
31. Paredes-Miranda, G.; Arnott, W.P.; Moosmüller, H.; Green, M.C.; Gyawali, M. Black Carbon Aerosol Concentration in Five Cities and Its Scaling with City Population. *Bull. Am. Meteorol. Soc.* **2013**, *94*, 41–50. [[CrossRef](#)]
32. Lim, S.; Kang, Y.; Lee, M.; Yoo, H.-J.; Lee, S.-S.; Lee, G.-H. Mass Concentration and Size Distribution of Refractory Black Carbon in Seoul during Summer. *J. Korean Soc. Atmos. Environ.* **2019**, *35*, 713–725. [[CrossRef](#)]
33. Pio, C.; Cerqueira, M.; Harrison, R.M.; Nunes, T.; Mirante, F.; Alves, C.; Oliveira, C.; Sanchez De La Campa, A.; Artíñano, B.; Matos, M. OC/EC ratio observations in Europe: Re-thinking the approach for apportionment between primary and secondary organic carbon. *Atmos. Environ.* **2011**, *45*, 6121–6132. [[CrossRef](#)]
34. Park, S.-S.; Jung, S.-A.; Gong, B.-J.; Cho, S.-Y.; Lee, S.-J. Characteristics of PM<sub>2.5</sub> haze episodes revealed by highly time-resolved measurements at an air pollution monitoring Supersite in Korea. *Aerosol Air Qual. Res.* **2013**, *13*, 957–976. [[CrossRef](#)]
35. Tian, J.; Ni, H.; Cao, J.; Han, Y.; Wang, Q.; Wang, X.; Chen, L.-W.A.; Chow, J.C.; Watson, J.G.; Wei, C.; et al. Characteristics of carbonaceous particles from residential coal combustion and agricultural biomass burning in China. *Atmos. Pollut. Res.* **2017**, *8*, 521–527. [[CrossRef](#)]
36. Day, M.C.; Zhang, M.; Pandis, S.N. Evaluation of the ability of the EC tracer method to estimate secondary organic carbon. *Atmos. Environ.* **2015**, *112*, 317–325. [[CrossRef](#)]
37. Morgan, W.T.; Allan, J.D.; Bower, K.N.; Highwood, E.J.; Liu, D.; Mcmeeking, G.R.; Northway, M.J.; Williams, P.I.; Krejci, R.; Coe, H. Airborne measurements of the spatial distribution of aerosol chemical composition across Europe and evolution of the organic fraction. *Atmos. Chem. Phys.* **2010**, *10*, 4065–4083.
38. Takegawa, N.; Kondo, Y.; Koike, M.; Chen, G.; Machida, T.; Watai, T.; Blake, D.R.; Streets, D.G.; Woo, J.-H.; Carmichael, G.R.; et al. Removal of NO<sub>x</sub> and NO<sub>y</sub> in Asian outflow plumes: Aircraft measurements over the western Pacific in January 2002. *JGR Atmos.* **2004**, *109*, D23S04.
39. Wang, Y.X.; Mcelroy, M.B.; Wang, T.; Palmer, P.I. Asian emissions of CO and NO<sub>x</sub>: Constraints from aircraft and Chinese station data. *J. Geophys. Res.* **2004**, *109*, D24304. [[CrossRef](#)]
40. Tang, W.; Emmons, L.K.; Arellano, A.F., Jr.; Gaubert, B.; Knote, C.; Tilmes, S.; Buchholz, R.R.; Pfister, G.G.; Diskin, G.S.; Blake, D.R.; et al. Source Contributions to Carbon Monoxide Concentrations During KORUS-AQ Based on CAM-chem Model Applications. *J. Geophys. Res. Atmos.* **2019**, *124*, 2796–2822. [[CrossRef](#)]
41. Lim, S.; Lee, M.; Lee, G.; Kim, S.; Yoon, S.; Kang, K. Ionic and carbonaceous compositions of PM<sub>10</sub>, PM<sub>2.5</sub> and PM<sub>1.0</sub> at Gosan ABC Superstation and their ratios as source signature. *Atmos. Chem. Phys.* **2012**, *12*, 2007–2024. [[CrossRef](#)]
42. Yu, X.; Ma, J.; An, J.; Yuan, L.; Zhu, B.; Liu, D.; Wang, J.; Yang, Y.; Cui, H. Impacts of meteorological condition and aerosol chemical compositions on visibility impairment in Nanjing, China. *J. Clean. Prod.* **2016**, *131*, 112–120. [[CrossRef](#)]

43. Tao, J.; Zhang, L.; Gao, J.; Wang, H.; Chai, F.; Wang, S. Aerosol chemical composition and light scattering during a winter season in Beijing. *Atmos. Environ.* **2015**, *110*, 36–44. [[CrossRef](#)]
44. Wang, Y.H.; Liu, Z.R.; Zhang, J.K.; Hu, B.; Ji, D.S.; Yu, Y.C.; Wang, Y.S. Aerosol physicochemical properties and implications for visibility during an intense haze episode during winter in Beijing. *Atmos. Chem. Phys.* **2015**, *15*, 3205–3215. [[CrossRef](#)]
45. Jordan, C.E.; Crawford, J.H.; Beyersdorf, A.J.; Eck, T.F.; Halliday, H.S.; Nault, B.A.; Chang, L.-S.; Park, J.; Park, R.; Lee, G.; et al. Investigation of factors controlling PM<sub>2.5</sub> variability across the South Korean Peninsula during KORUS-AQ. *Sci. Anthr.* **2020**, *8*, 1026–2325. [[CrossRef](#)] [[PubMed](#)]